

Phase diagram and physical properties of $\text{NaFe}_{1-x}\text{Cu}_x\text{As}$ single crystals

A. F. Wang, J. J. Lin, P. Cheng, G. J. Ye, F. Chen, J. Q. Ma, X. F. Lu, B. Lei, X. G. Luo and X. H. Chen*
*Hefei National Laboratory for Physical Science at Microscale and Department of Physics,
 University of Science and Technology of China, Hefei,
 Anhui 230026, People's Republic of China*

A series of high quality $\text{NaFe}_{1-x}\text{Cu}_x\text{As}$ single crystals has been grown by a self-flux technique, which were systematically characterized via structural, transport, thermodynamic, and high pressure measurements. Both the structural and magnetic transitions are suppressed by Cu doping, and bulk superconductivity is induced by Cu doping. Superconducting transition temperature (T_c) is initially enhanced from 9.6 to 11.5 K by Cu doping, and then suppressed with further doping. A phase diagram similar to $\text{NaFe}_{1-x}\text{Co}_x\text{As}$ is obtained except that insulating instead of metallic behavior is observed in extremely overdoped samples. T_c 's of underdoped, optimally doped, and overdoped samples are all notably enhanced by applying pressure. Although a universal maximum transition temperature (T_c^{max}) of about 31 K under external pressure is observed in underdoped and optimally doped $\text{NaFe}_{1-x}\text{Co}_x\text{As}$, T_c^{max} of $\text{NaFe}_{1-x}\text{Cu}_x\text{As}$ is monotonously suppressed by Cu doping, suggesting that impurity potential of Cu is stronger than Co in NaFeAs. The comparison between Cu and Co doping effect in NaFeAs indicates that Cu serves as an effective electron dopant with strong impurity potential, but part of the doped electrons are localized and do not fill the energy bands as predicted by the rigid-band model.

PACS numbers: 74.70.Xa, 74.62.-c, 74.25.F-, 74.62.Dh

I. INTRODUCTION

The discovery of iron-based superconductors gives another opportunity to study the physics of high-temperature superconductivity besides the cuprates.¹⁻³ The parent compounds of iron-based superconductors are antiferromagnetic semimetals, and superconductivity can be induced by hole, electron doping or applying pressure. For example, superconductivity was induced in BaFe_2As_2 by the doping of Co, Ni, and Cu.^{4,5} In the case of Co and Ni doping, the doped electron numbers predicted by rigid band model are x and $2x$, respectively. The study on phase diagram of $\text{Ba}(\text{Fe}_{1-x}\text{Co}_x)_2\text{As}_2$ and $\text{Ba}(\text{Fe}_{1-x}\text{Ni}_x)_2\text{As}_2$ by angle-resolved photoemission spectroscopy (ARPES) indicates that the doped electron number roughly follows the rigid-band model.⁶ Therefore, it is natural to expect that superconductivity could be induced by Cu doping and the doped electron number is $3x$. However, superconductivity was observed in a very narrow range of doping in $\text{Ba}(\text{Fe}_{1-x}\text{Cu}_x)_2\text{As}_2$,⁵ and no superconductivity was observed in $\text{Sr}(\text{Fe}_{1-x}\text{Cu}_x)_2\text{As}_2$.⁷

Although the doping effect of Co and Ni is clear now, the role of Cu doping is still under debate. X-ray photoelectron spectroscopy (XPS) and x-ray absorption (XAS) measurements show that Cu $3d$ states locate at the bottom of the valence band in a localized $3d^{10}$ shell, so that the formal valence state of Cu is +1 and the substitution of Fe^{2+} by Cu^{1+} results in hole doping.⁷⁻⁹ The theoretical and experimental studies on SrCu_2As_2 , the end member of $\text{Sr}(\text{Fe}_{1-x}\text{Cu}_x)_2\text{As}_2$ series, indicate that it is an sp -band

metal with hole-type carries dominate and Cu in the non-magnetic $3d^{10}$ electronic configuration corresponds to the valence state Cu^{1+} ,^{7,10,11} which further supports the result of XPS and XAS. In addition, the doping effect of Cu is similar to that of Mn, which is also considered as hole doping and no superconductivity has been found.¹² On the other hand, electron doping by Cu was proved by ARPES,⁶ and further confirmed by hall measurement on $\text{Ba}_{0.6}\text{K}_{0.4}(\text{Fe}_{1-x}\text{Cu}_x)_2\text{As}_2$.¹³ Similar superconducting dome to that of $\text{Ba}(\text{Fe}_{1-x}\text{Co}_x)_2\text{As}_2$ was observed in the phase diagram of $\text{Ba}(\text{Fe}_{1-x-y}\text{Co}_x\text{Cu}_y)_2\text{As}_2$ ($x \sim 0.022$ and $x \sim 0.047$),⁵ indicating the similar doping effect between Co and Cu, and suggesting electron doping induced by Cu substitution. To reconcile this controversial situation, it is of great interest to further investigate the Cu doping effect in other family of iron-pnictide superconductors.

Besides BaFe_2As_2 , high quality of NaFeAs single crystal is also available now, which turns out to be suitable for studying the Cu doping effect. NaFeAs is regarded as a filamentary superconductor, and the superconductivity cannot be detected by specific heat. By substituting Co or Ni on Fe sites, bulk superconductivity was obtained.^{14,15} The Ni doping doubles the amount of electron doping of Co,¹⁴ which follows the rigid band model. Moreover, it has been reported that T_c of analogous compound $\text{LiFe}_{1-x}\text{Cu}_x\text{As}$ is suppressed linearly by Cu doping.¹⁶ Hence, we study the role of Cu doping in $\text{NaFe}_{1-x}\text{Cu}_x\text{As}$, and compare it with the effect of Cu doping in BaFe_2As_2 and LiFeAs . In this paper, we report the study on the physical properties and phase diagram of $\text{NaFe}_{1-x}\text{Cu}_x\text{As}$ by measuring x-ray diffraction (XRD), resistivity, magnetic susceptibility, Hall coefficient, specific heat, and high pressure. A phase diagram

*Corresponding author; Electronic address: chenxh@ustc.edu.cn

similar to $\text{NaFe}_{1-x}\text{Co}_x\text{As}$ is established. The comparison of the physical properties and phase diagrams between $\text{NaFe}_{1-x}\text{Cu}_x\text{As}$ and $\text{NaFe}_{1-x}\text{Co}_x\text{As}$ clearly indicates that Cu doping is electron doping and the electron concentration deviates from the expected $3x$. The deviation can be explained that part of the doped electrons fill the impurity band which is located deep below the Fermi level (E_F) and do not fill the energy bands as predicted by the rigid-band model.^{6,9}

II. EXPERIMENTAL DETAILS

A series of $\text{NaFe}_{1-x}\text{Cu}_x\text{As}$ single crystals was grown by adopting the NaAs flux method. Its growth procedure resembles to that of $\text{NaFe}_{1-x}\text{Co}_x\text{As}$, and the details can be found in our previous work.¹⁵ XRD was performed on a Smartlab-9 diffractometer (Rikagu) from 10° to 70° , with a scanning rate of 6° per minute. The actual chemical composition of the single crystal was determined by energy dispersive x-ray spectroscopy (EDX). The Cu content x hereafter is the actual composition determined by EDX. The resistivity and specific heat measurements were carried out by using the PPMS-9T (Quantum Design), and resistivity down to 50 mK were measured in a dilution refrigerator on PPMS. The magnetic susceptibility was measured using a vibrating sample magnetometer (VSM) (Quantum Design). The Hall coefficient was measured on PPMS with the four-terminal ac technique by switching the polarity of the magnetic field $H // c$ to remove any magnetoresistive components due to the misalignment of the voltage contacts.¹⁷ The pressure was generated in a Teflon cup filled with Daphne Oil 7373, which was inserted into a Be-Cu pressure cell, and the pressure applied in the resistivity measurement was determined by shifting the superconducting transition temperature of pure Sn.

III. RESULTS

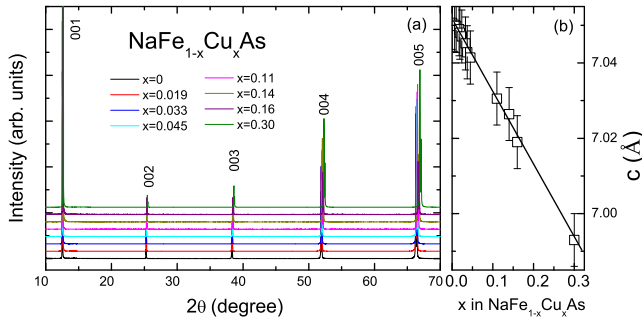


FIG. 1: (color online). (a) Selected XRD patterns for the $\text{NaFe}_{1-x}\text{Cu}_x\text{As}$ single crystals. (b) Doping dependence of the c -axis parameter.

A. X-ray diffraction

Figure 1(a) shows the selected single-crystalline XRD patterns for the $\text{NaFe}_{1-x}\text{Cu}_x\text{As}$ single crystals. Only $(00l)$ reflections can be recognized, indicating that the crystals are well orientated along the c axis. The lattice parameter c is estimated from the $(00l)$, and the evolution of all the single crystals' lattice parameter c with the doping level is shown in Fig. 1(b). The lattice parameter c decreases with increasing doping concentration, which roughly obeys the Vegard's law. Comparing with undoped NaFeAs , the amplitude of lattice parameter change is about 0.8% with Cu doping concentration up to 0.30, a little smaller than that of Co doped NaFeAs with the same doping level.^{14,15}

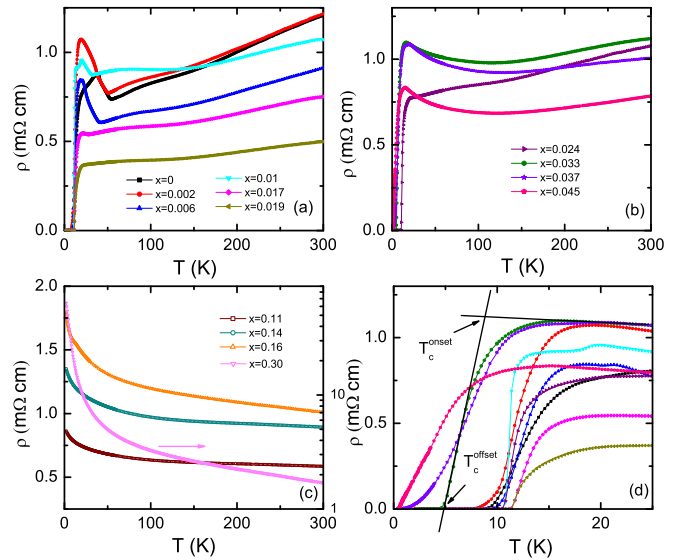


FIG. 2: (color online). (a)-(c) Temperature dependence of in-plane resistivity for $\text{NaFe}_{1-x}\text{Cu}_x\text{As}$ single crystals. (d) Enlargement of the low temperature resistivity in panels (a) and (b). The criteria used to determine the onset and offset temperature for the superconducting transitions is also shown in (d).

B. Electrical resistivity

The temperature dependence of in-plane electrical resistivity for $\text{NaFe}_{1-x}\text{Cu}_x\text{As}$ single crystals are shown in Fig. 2. To make the graphs easier to read, the data are grouped into three sets. The resistivity at room temperature is about 0.4-1.7 mΩ cm.^{15,18} The error bar of the absolute resistivity is relatively large comparing to the evolution of resistivity caused by the doping effect, which is mainly coming from the uncertainty of geometric factor. So we cannot observe a systematic evolution of the room temperature resistivity in the whole doping range. The superconducting transitions for most of the samples

are quite broad and the onset is very round, so we define T_c^{offset} as T_c , as shown in Fig. 2(d). T_c stands for T_c^{offset} for convenience hereafter. The kinks associated with the structural/spin density wave (SDW) transition are clearly resolved in the low temperature resistivity of underdoped crystals.¹⁹ We use the same criteria to define the structural and SDW transition as described in Ref. 15.

The structural and SDW transitions are progressively suppressed with increasing Cu concentration, similar to $\text{NaFe}_{1-x}\text{Co}_x\text{As}$. T_c increases slightly with Cu doping in the underdoped region. The maximum T_c about 11.5 K is reached at $x = 0.019$, but the amplitude of T_c enhancement (2K) is much smaller than that in Co doped NaFeAs (10K). T_c decreases quickly with further increasing Cu doping, and no trace of superconducting transition is observed in crystals with doping concentration larger than 0.045. Metal-insulator transition is observed in the crystals with doping level higher than 0.033. Ultimately, insulating behavior in the whole temperature range is observed in the extremely overdoped crystals, which is quite different from the metallic behavior in extremely overdoped $\text{NaFe}_{1-x}\text{Co}_x\text{As}$.¹⁵ A weak semiconducting behavior is also observed in $\text{Ba}(\text{Fe}_{1-x}\text{Cu}_x)_2\text{As}_2$ and $\text{Sr}(\text{Fe}_{1-x}\text{Cu}_x)_2\text{As}_2$.^{5,7} In addition, when $\sim 4\%$ Fe was substituted by Cu, a metal-insulator transition was observed in $\text{Fe}_{1.01-x}\text{Cu}_x\text{Se}$.^{20,21} It is reported that the insulator phase of $\text{Fe}_{1.01-x}\text{Cu}_x\text{Se}$ is an Anderson localized system arising from disorder rather than a conventional semiconductor.²² Whether the metal-insulator transition in $\text{NaFe}_{1-x}\text{Cu}_x\text{As}$ and $\text{Fe}_{1.01-x}\text{Cu}_x\text{Se}$ have common origin need further investigation.

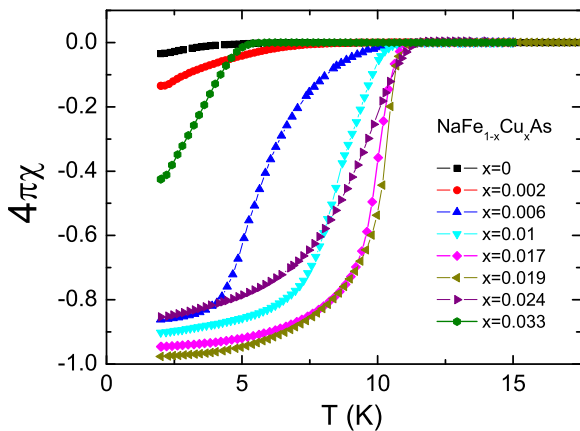


FIG. 3: (color online). Temperature dependent magnetic susceptibility for $\text{NaFe}_{1-x}\text{Cu}_x\text{As}$ with magnetic field 10 Oe

C. Magnetic susceptibility

Figure 3 shows the zero-field-cooling (ZFC) magnetic susceptibility taken at 10 Oe with H perpendicular to

the c axis for the superconducting $\text{NaFe}_{1-x}\text{Cu}_x\text{As}$ single crystals. As reported previously, a tiny diamagnetic signal was observed below 9 K in undoped NaFeAs .¹⁵ With Cu doping, the superconducting shielding fraction rises rapidly. Bulk superconductivity with large shielding fraction is observed in the composition range of 0.006 \sim 0.024, indicating that Cu doping is beneficial to the superconductivity of NaFeAs . T_c inferred from the diamagnetic signal is consistent with that determined by resistivity measurement. As shown in Fig. 3, $x = 0.019$ is the optimally doped composition with maximum T_c and largest shielding fraction. Both shielding fraction and T_c decrease with further Cu doping, and no diamagnetic signal above 2 K is detected in samples with the Cu doping level higher than 0.033.

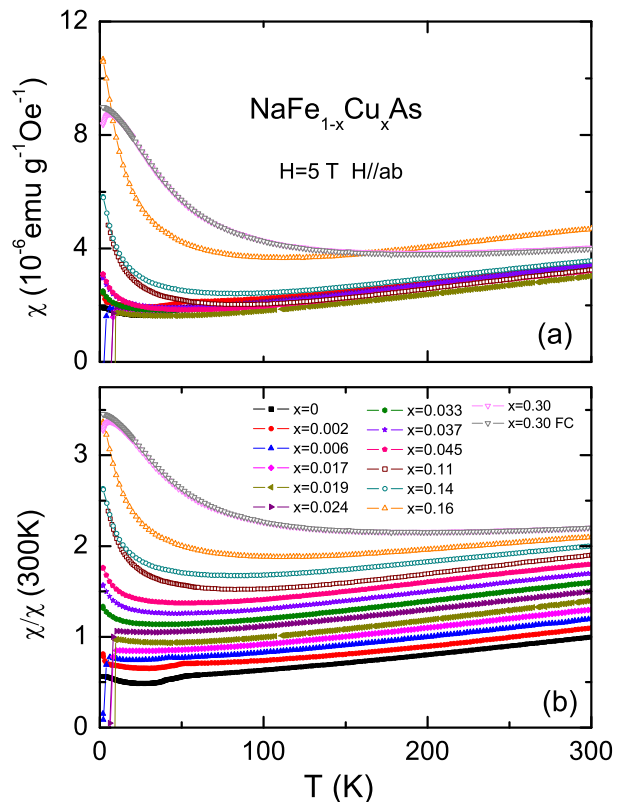


FIG. 4: (color online). (a) Temperature dependence of normal state magnetic susceptibility for $\text{NaFe}_{1-x}\text{Cu}_x\text{As}$ under a magnetic field of 5 T. (b) Temperature dependence of the normalized magnetic susceptibility, which is shifted upward by 0.1 for clarity.

Figure 4 (a) presents the normal state in-plane magnetic susceptibility for $\text{NaFe}_{1-x}\text{Cu}_x\text{As}$ under a magnetic field of 5 T. The magnitude and behavior is similar to that in Co doped NaFeAs .¹⁵ Because the magnitude of χ does not change much in the doping range up to 0.014 (about 15%), the normalized susceptibility is shown in Fig. 4(b) for clarity. All the magnetic susceptibility is taken under zero-field-cooled (ZFC) mode, and a field-

cooled (FC) susceptibility of $\text{NaFe}_{0.70}\text{Cu}_{0.30}\text{As}$ is also presented. Rapid drops associated with superconducting transition can still be observed at low temperature for the superconducting samples. Kinks corresponding to the structural and SDW transitions are observed in the undoped and underdoped samples, which are suppressed with Cu doping and consistent with the observation of resistivity. It is worth noting that χ shows an almost linear temperature dependence in high temperature for concentration up to 0.16. The slope of the linear dependence of high-temperature susceptibility slightly decreases with Cu doping, similar to Co doping.¹⁵ The linear temperature dependence of high temperature susceptibility is a common feature in iron-based superconductors, which has been observed in $\text{NaFe}_{1-x}\text{Co}_x\text{As}$,¹⁵ $\text{Ba}(\text{Fe}_{1-x}\text{Co}_x)_2\text{As}_2$,²³ and $\text{LaFeAsO}_{1-x}\text{F}_x$.²⁴ An explanation based on the J_1 - J_2 model of localized spins ascribes this behavior to the spin fluctuations arising from the local SDW correlation.²⁵ It is also argued that the behavior can be explained based on the spin susceptibility of a 2D Fermi-liquid with nearly nested electron and hole pockets of the Fermi surface.²⁶ There is a Curie-Weiss like upturn in the low temperature magnetic susceptibility of overdoped $\text{NaFe}_{1-x}\text{Cu}_x\text{As}$, which has been reported in many Fe-based superconductors.^{5,15,27,28} The susceptibility upturn is usually attributed to extrinsic origin, such as defects or impurities. A small separation between the ZFC and FC occurs at $\text{NaFe}_{0.70}\text{Cu}_{0.30}\text{As}$, which is considered as spin glass transition.⁷

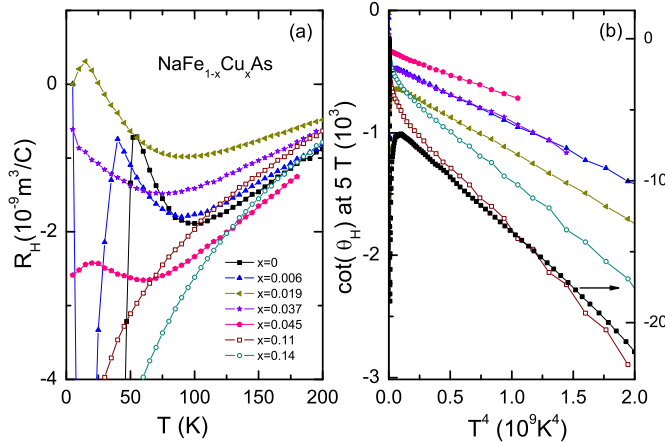


FIG. 5: (color online). (a) Temperature dependence of the Hall coefficient R_H for selected $\text{NaFe}_{1-x}\text{Cu}_x\text{As}$ single crystals. (b) The $\cot\theta_H$ of $\text{NaFe}_{1-x}\text{Cu}_x\text{As}$ single crystals plotted in power-law temperature scale. The legends in (b) are same as (a)

D. Hall effect

Figure 5(a) shows the temperature dependence of Hall coefficients for selected single crystals of $\text{NaFe}_{1-x}\text{Cu}_x\text{As}$.

The sharp drop in the $x = 0$ and $x = 0.006$ single crystals is due to structural transition, and the temperature of the transition determined from resistivity, magnetic susceptibility, and Hall coefficient is consistent with each other. The negative Hall coefficient of all the single crystals indicate that the dominated carrier is electron. A systematic evolution is observed on the absolute value of Hall coefficient at 200 K. The value decreases with Cu doping up to optimally doped crystal with $x=0.019$, and then increases with further Cu doping. Due to the multi-band effect and different mobility of electron and hole carries, the Hall behavior is complex. If we simply take the single band expression $n_H = 1/(eR_H)$,²⁹ the behavior of Hall coefficient of $\text{NaFe}_{1-x}\text{Cu}_x\text{As}$ indicates that the Cu doping is electron doping, similar to that of Co doping in $\text{NaFe}_{1-x}\text{Co}_x\text{As}$.¹⁵ As the Cu doping, Hall coefficients of $\text{Ba}_{0.6}\text{K}_{0.4}(\text{Fe}_{1-x}\text{Cu}_x)_2\text{As}_2$ gradually change from positive values to negative values, clearly showing electron carriers are introduced. The result of Hall measurement on $\text{NaFe}_{1-x}\text{Cu}_x\text{As}$ is similar to the result of $\text{Ba}_{0.6}\text{K}_{0.4}(\text{Fe}_{1-x}\text{Cu}_x)_2\text{As}_2$.¹³

As shown in Fig. 5(b), The Hall angle is plotted as $\cot\theta_H = \rho/\rho_{xy}$ vs T^4 , where ρ is in-plane resistivity and ρ_{xy} is Hall resistivity. It has been reported that $\cot\theta_H$ shows power-law temperature dependence for all the single crystals of $\text{NaFe}_{1-x}\text{Co}_x\text{As}$: T^4 for the parent compound, approximately T^3 for the superconducting crystals and T^2 for the heavily overdoped non-superconducting sample.¹⁷ But T^β -dependent $\cot\theta_H$ with $\beta \approx 4$ is observed in these $\text{NaFe}_{1-x}\text{Cu}_x\text{As}$ single crystals. This value is different from $\text{NaFe}_{1-x}\text{Co}_x\text{As}$, $\text{Ba}(\text{Fe}_{1-x}\text{Co}_x)_2\text{As}_2$,³⁰ and hole doped cuprates,³¹ but similar to electron-doped cuprates.³² Since the T^4 -dependence in cuprate is interpreted by the multi-band effect with different contributions from various bands, the different power law dependence between $\text{NaFe}_{1-x}\text{Cu}_x\text{As}$ and $\text{NaFe}_{1-x}\text{Co}_x\text{As}$ indicates the different band evolution of NaFeAs by Cu/Co doping.

E. Specific heat

To verify the bulk thermodynamic nature of the superconducting transition, specific heat measurement were performed on optimally doped $\text{NaFe}_{0.981}\text{Cu}_{0.019}\text{As}$, as shown in Fig. 6. Remarkable jump in specific heat corresponding to superconducting transition is observed, while no anomaly can be observed on NaFeAs single crystal. The obvious jump in specific heat suggests that bulk superconductivity in NaFeAs is obtained by Cu doping.

The red line is the best fit of the normal state specific heat between 13 and 30 K by $C_P = \gamma_n T + \beta T^3 + \eta T^5$, where $\gamma_n T$ and $\beta T^3 + \eta T^5$ are electron and phonon contributions, respectively. It is found that $\gamma_n = 7.44 \text{ mJ mol}^{-1} \text{ K}^{-2}$, $\beta = 0.238 \text{ mJ mol}^{-1} \text{ K}^{-4}$, and $\eta = -5.00 \times 10^{-5} \text{ mJ mol}^{-1} \text{ K}^{-6}$. The estimated Debye temperature is 290 K, almost same to the corresponding value for $\text{NaFe}_{0.972}\text{Co}_{0.028}\text{As}$.¹⁵ $\Delta C_p/T_c$ at

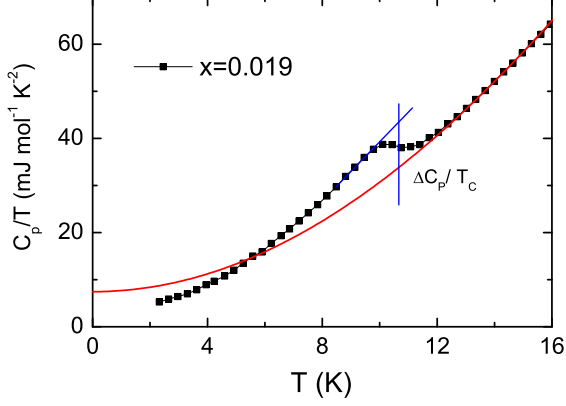


FIG. 6: (color online). Specific heat of optimally doped $\text{NaFe}_{0.981}\text{Cu}_{0.019}\text{As}$. Blue lines show how the $\Delta C_p/T_c$ was determined. The red line is the best fit of the specific heat between 13 and 30 K. (Only data below 16 K is shown for clarity)

$T_c = 10.65$ K is estimated to $9.85 \text{ mJ mol}^{-1} \text{ K}^{-2}$ by isentropic construction sketched in Fig. 6. The value roughly follow the expanded BNC scaling, which is proposed by Bud'ko, Ni, and Canfield (BNC) and expanded by J. S. Kim *et al.*^{33,34} The BNC scaling is considered as a simple test of whether a material belongs to the iron-based superconductors.³⁵ So the pairing symmetry of $\text{NaFe}_{0.981}\text{Cu}_{0.019}\text{As}$ may be similar to $\text{Ba}(\text{Fe}_{0.925}\text{Co}_{0.075})_2\text{As}_2$ and $\text{NaFe}_{0.972}\text{Co}_{0.028}\text{As}$. It has been reported that $\Delta C_p/\gamma_n T_c = 2.11$ in $\text{NaFe}_{0.972}\text{Co}_{0.028}\text{As}$.¹⁵ Based on the data obtained above, $\Delta C_p/\gamma_n T_c$ in $\text{NaFe}_{0.981}\text{Cu}_{0.019}\text{As}$ is estimated to 1.32, a little smaller than 1.43 expected for weak-coupling BCS superconductor. The different value between optimally Cu and Co doped NaFeAs suggests that the coupling strength in Cu doped NaFeAs is weaker than Co doped. As a result, $\text{NaFe}_{0.981}\text{Cu}_{0.019}\text{As}$ may be a two band s-wave superconductor with a weaker coupling strength.

F. Phase diagram

The $T-x$ phase diagram of $\text{NaFe}_{1-x}\text{Cu}_x\text{As}$ is plotted in Fig. 7, where T_s , T_{SDW} , and T_c stand for structural, SDW, and superconducting transition, respectively. The data in Fig. 7 is obtained from resistivity, which is consistent with magnetic susceptibility, Hall, and specific heat measurements. As the Cu doping, both structural and SDW transitions are progressively suppressed to low temperature, and T_c is enhanced slightly from 9.6 K in NaFeAs to 11.5 K in optimally Cu doped NaFeAs . T_c decreases with Cu concentration in overdoped region, and metal-insulator transition is observed in the normal state resistivity of overdoped superconducting samples. Extremely overdoped samples exhibit insulating behavior,

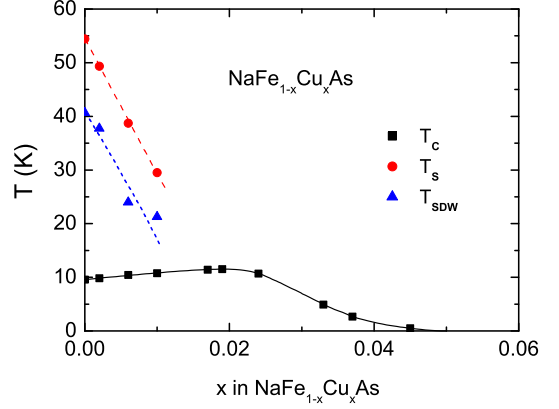


FIG. 7: (color online). $T-x$ phase diagram of $\text{NaFe}_{1-x}\text{Cu}_x\text{As}$. Lines are guides to the eye.

which is different from the overdoped nonsuperconducting $\text{NaFe}_{1-x}\text{Co}_x\text{As}$, where metallic behavior is observed. A weak semiconductor behavior is also observed on overdoped $\text{Ba}(\text{Fe}_{1-x}\text{Cu}_x)_2\text{As}_2$ and $\text{Sr}(\text{Fe}_{1-x}\text{Cu}_x)_2\text{As}_2$.^{5,7} Although the magnitude of T_c enhancement of NaFeAs is only 1.9 K by Cu doping, the negligible small shielding fraction is greatly enhanced to nearly 100%. The full shielding fraction indicates Cu doping is beneficial for the superconductivity of NaFeAs , contrast to the case of $\text{LiFe}_{1-x}\text{Cu}_x\text{As}$.¹⁶ But the maximum T_c is obviously lower than 20 K in $\text{NaFe}_{1-x}\text{Co}_x\text{As}$ under ambient pressure, the maximum T_c may be suppressed by stronger impurity potential of Cu. Microscopic coexistence of SDW and superconductivity has been proved by scanning tunneling microscopy (STM) in underdoped $\text{NaFe}_{1-x}\text{Co}_x\text{As}$.³⁶ As shown in Fig. 7, superconductivity also coexists with SDW in underdoped $\text{NaFe}_{1-x}\text{Cu}_x\text{As}$.

G. Pressure effects

Resistivity measurements under pressure were performed in underdoped sample with $x = 0.006$, optimally doped $x = 0.019$, and overdoped $x = 0.037$ samples. As shown in Fig. 8 (a), for underdoped single crystal with $x = 0.006$, the resistivity upturn associated with the structural or SDW transitions is suppressed to low temperature by pressure and eventually become indistinguishable. T_c initially increased by applying pressure, and maximum $T_c = 26.2$ K is observed at 2.2 GPa, the T_c decreases with further increasing pressure, the data is summarized in Fig. 8(b). For optimally doped and overdoped samples, where structural and SDW transitions have been suppressed by Cu doping, T_c are monotonously enhanced up to the maximum pressure in our measurement.

As shown in Figs. 8(d) and 8(f), the $T_c^{\text{max}} = 24.6$ and 12.9 K are obtained for $x = 0.019$ and $x = 0.037$,

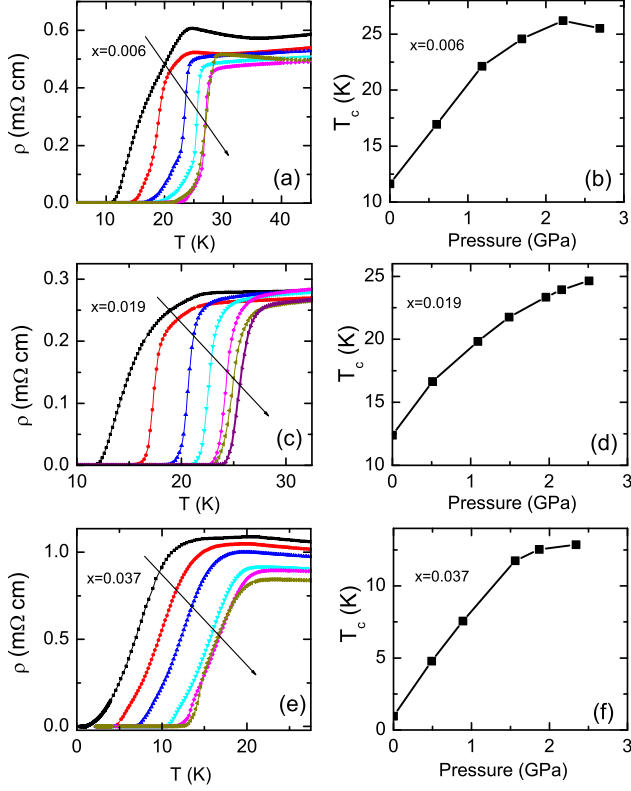


FIG. 8: (color online). Left panels: in-plane resistivity of $\text{NaFe}_{1-x}\text{Cu}_x\text{As}$ ($x=0.006$ (a), 0.019 (c) and 0.037 (e)) under various pressures, arrows indicate the direction of the increasing pressure. Right panels: the $T(p)$ phase diagrams of the samples corresponding to the left panels.

respectively. The pressure coefficient between ambient pressure and the pressure at which T_c reaches its maximum is 5.2 , 4.9 , and 5.1 K GPa^{-1} , comparable to the optimally doped and overdoped $\text{NaFe}_{1-x}\text{Co}_x\text{As}$.³⁷

The maximum transition temperature (T_c^{\max}) of $\text{NaFe}_{1-x}\text{Co}_x\text{As}$ and $\text{NaFe}_{1-x}\text{Cu}_x\text{As}$ obtained under pressure is plotted on Fig. 9. As shown in Fig. 9, the maximum T_c obtained by combining the effect of doping and pressure in $\text{NaFe}_{1-x}\text{Cu}_x\text{As}$ decreases with Cu concentration, contrast to the pressure effect on $\text{NaFe}_{1-x}\text{Co}_x\text{As}$, where maximum T_c about 31 K is observed from undoped to optimally doped samples.³⁷ Substitution of Fe by other transition metal can induce carries as well as impurities. Because both Co and Cu can dope electron into NaFeAs , it is mainly the impurity effect that responds for the different T_c^{\max} evolution as a function of doping. If we only consider the impurity effect on the maximum transition temperature of NaFeAs , T_c -suppression rate for Cu is $\Delta T_c/\text{Cu-1\%} = -4.3$ K, slightly larger than -3.5 K in $\text{Ba}_{0.6}\text{K}_{0.4}(\text{Fe}_{1-x}\text{Cu}_x)_2\text{As}_2$,¹³ but much larger than -0.7 K in $\text{NaFe}_{1-x}\text{Co}_x\text{As}$ with similar doping concentration. The large T_c -suppression rate of $\text{NaFe}_{1-x}\text{Cu}_x\text{As}$ suggests that the impurity potential of Cu is stronger

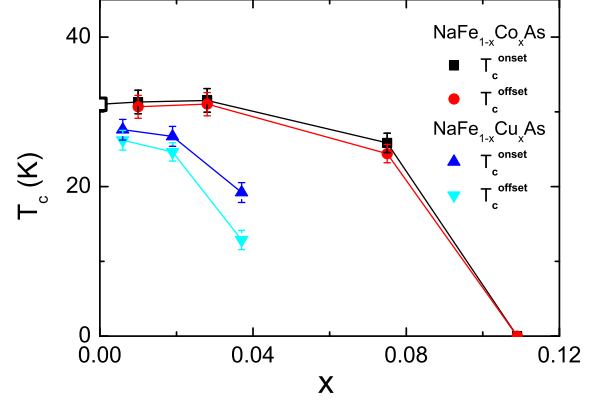


FIG. 9: (color online). T_c^{\max} of $\text{NaFe}_{1-x}\text{Co}_x\text{As}$ and $\text{NaFe}_{1-x}\text{Cu}_x\text{As}$ plotted as functions of the Co/Cu substitution, x . The open black symbol represents the T_c^{\max} of NaFeAs reported by Zhang *et al.*⁴⁴ The data of $\text{NaFe}_{1-x}\text{Co}_x\text{As}$ is taken from Ref. 37.

than Co in NaFeAs .

H. Anisotropy of the upper critical field

In Fig. 10, we present the temperature dependence of resistivity for $\text{NaFe}_{1-x}\text{Cu}_x\text{As}$ ($x=0.006$, 0.019) under various magnetic fields. The transition temperature of superconductivity (the criteria is shown in Fig. 2(d)) is suppressed gradually and the transition is broadened with increasing magnetic field. The effect of magnetic field is much larger when the field is applied along the c axis of the single crystals instead of within the ab plane. For underdoped sample $\text{NaFe}_{0.994}\text{Cu}_{0.006}\text{As}$, the positive magnetoresistance appears well below the temperature which is defined as the SDW transition. The similar phenomenon was observed in NaFeAs single crystal,³⁸ and confirmed by neutron scattering.¹⁹ Temperature dependent H_{c2} curves for $\text{NaFe}_{0.994}\text{Cu}_{0.006}\text{As}$ and $\text{NaFe}_{0.981}\text{Cu}_{0.019}\text{As}$ is shown in Figs. 7(c) and 7(f), respectively. In order to determine the upper critical field in the low-temperature region, we adopt the Werthamer-Helfand-Hohenberg (WHH) formula $H_{c2}(0) = 0.693[-(dH_{c2}/dT)]_{T_c}T_c$ for single band BCS superconductor. We obtain $[-(dH_{c2}^{ab}/dT)]_{T_c} = 4.23$ T/K and $[-(dH_{c2}^c/dT)]_{T_c} = 2.24$ T/K at $T_c = 10.40$ K from Fig. 7(c) for $\text{NaFe}_{0.994}\text{Cu}_{0.006}\text{As}$, so the $H_{c2}(0)$ can be estimated to be 30 and 16 T with the field parallel and perpendicular to the ab plane, respectively. In the same way, $H_{c2}^{ab}(0) = 49$ T and $H_{c2}^c(0) = 22$ T are obtained for $\text{NaFe}_{0.981}\text{Cu}_{0.019}\text{As}$ single crystal. As a result, the anisotropy parameter $\gamma_H = H_{c2}^{ab}(0)/H_{c2}^c(0)$ can be estimated to be 1.88 and 2.22 for $\text{NaFe}_{0.994}\text{Cu}_{0.006}\text{As}$ and $\text{NaFe}_{0.981}\text{Cu}_{0.019}\text{As}$, respectively. The smaller anisotropy γ_H of underdoped samples than the overdoped samples has also observed on

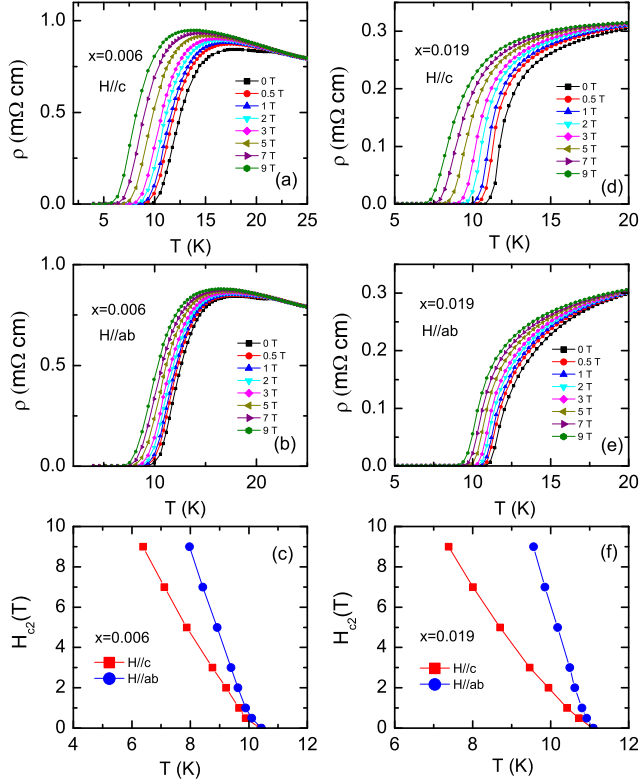


FIG. 10: (color online). The temperature dependence of resistivity for underdoped $\text{NaFe}_{0.994}\text{Cu}_{0.006}\text{As}$ (a)-(b), and optimally doped $\text{NaFe}_{0.981}\text{Cu}_{0.019}\text{As}$ (d)-(e) crystals with the magnetic field parallel and perpendicular to the c axis, respectively. (c) and (f) The temperature dependence of H_{c2} for $\text{NaFe}_{0.994}\text{Cu}_{0.006}\text{As}$ and $\text{NaFe}_{0.981}\text{Cu}_{0.019}\text{As}$, respectively.

$\text{Ba}(\text{Fe}_{1-x}\text{Co}_x)_2\text{As}_2$, where $\sim 50\%$ smaller anisotropy was found in underdoped region.³⁹ These anisotropy values are close to 2.25 - 2.35 for $\text{NaFe}_{1-x}\text{Co}_x\text{As}$,¹⁸ and a little larger than 1.7 - 1.86 in $\text{Ba}_{0.60}\text{K}_{0.40}\text{Fe}_2\text{As}_2$ and $\text{Fe}(\text{Se}, \text{Te})$ system,^{40,41} but smaller than 5 - 9 in $\text{NdFeAsO}_{1-x}\text{F}_x$.⁴²

IV. DISCUSSION

Although the T_c of optimally doped $\text{NaFe}_{1-x}\text{Cu}_x\text{As}$ is lower than that in $\text{NaFe}_{1-x}\text{Co}_x\text{As}$ and the superconducting dome is much narrower than that of $\text{NaFe}_{1-x}\text{Co}_x\text{As}$, the overall phase diagram of $\text{NaFe}_{1-x}\text{Cu}_x\text{As}$ is similar to those of $\text{NaFe}_{1-x}\text{Co}_x\text{As}$ and $\text{Ba}(\text{Fe}_{1-x-y}\text{Co}_x\text{Cu}_y)_2\text{As}_2$ ($x \sim 0.022$ and 0.047).^{5,15} This indicates that the similar doping effect of Cu and Co. As a result, the Cu doping definitely introduces electron carriers into $\text{NaFe}_{1-x}\text{Cu}_x\text{As}$. The main difference between Cu and Co doped NaFeAs lies in that the insulating phase instead of the metallic phase is observed in the extremely overdoped samples, indicating Cu doping effect distinct from Co except carries doping effect.

According to the comparison of the phase diagrams for $\text{Ba}(\text{Fe}_{1-x}\text{TM}_x)_2\text{As}_2$ ($\text{TM} = \text{Co}, \text{Ni}, \text{Cu}, \text{ and } \text{Co/Cu}$), the narrow superconducting dome of $\text{Ba}(\text{Fe}_{1-x}\text{Cu}_x)_2\text{As}_2$ has been interpreted that too many electrons have been added when the structural/antiferromagnetic phase transitions are suppressed low enough.⁵ But recent ARPES result on $\text{Ba}(\text{Fe}_{1-x}\text{TM}_x)_2\text{As}_2$ ($\text{TM} = \text{Co}, \text{Ni}, \text{ and } \text{Cu}$) suggests that although electrons are indeed doped, part of them may be localized and do not fill the energy bands as predicted by the rigid-band model.⁶ Theory calculation found that the substitution with strong impurity potential induces an impurity band split-off below the original host band, which reduces the electron occupy from the host band, result in decrease of the electron occupation.⁴⁵⁻⁴⁷ ARPES and density functional theory (DFT) studies found that the impurity potential of the substituted atoms enhances from Co, Ni, to Cu.^{6,45,48} As a result, the number of electron doped by Cu is less than the value expected from the simple rigid-band model.

As also suggested by high pressure measurement, the impurity effect of Cu is stronger than Co. The dome of superconductivity is mainly controlled by the balance of carrier concentration and impurity scattering induced by the dopants. So the narrow or even absence of superconducting dome in the phase diagram of Cu doped BaFe_2As_2 arises from that enough carriers are doped and so many impurities are induced. Therefore, the expanded superconducting dome of $\text{Ba}(\text{Fe}_{1-x-y}\text{Co}_x\text{Cu}_y)_2\text{As}_2$ ($x \sim 0.022$ and 0.047) than $\text{Ba}(\text{Fe}_{1-x}\text{Cu}_x)_2\text{As}_2$ can be understood that fewer carriers are needed when BaFe_2As_2 have been electron doped with Co. While in NaFeAs , whose structural/SDW transition temperature is much lower than BaFe_2As_2 , fewer electrons are required to suppress SDW and induce superconductivity. Therefore, Cu doping can provide enough carriers to map out a phase diagram similar to $\text{NaFe}_{1-x}\text{Co}_x\text{As}$ and $\text{Ba}(\text{Fe}_{1-x}\text{Co}_x)_2\text{As}_2$. Meanwhile, as the Cu concentration further increases, density of States (DOS) at E_F is gradually removed by the impurity band induced by Cu doping. As a result, metal-insulator transition is observed as a function of doping.

This scenario can also explain the contradiction between results of XPS/XAS and ARPES. Since Cu $3d$ states are located deeper below the E_F than Co,^{6,9,45} the extra d electrons for Cu almost totally locate around the substituted site. Hence, closed $3d$ shell is observed by XPS and XAS, although there is a little delocated electron introduced by Cu dopant. It is found that substitutions of Cu for Fe in $(\text{Ba}, \text{Sr})\text{Fe}_2\text{As}_2$ at low level result in electron doping, while in SrCu_2As_2 , the end member of $\text{Sr}(\text{Fe}_{1-x}\text{Cu}_x)_2\text{As}_2$, is an sp -band metal with hole-type carries dominate.^{6,7,11} The contradictory result has been interpreted that there is a crossover between electron and hole doping with increasing x , which is induced by tetragonal (T) to collapsed tetragonal (cT) phase transition as a function of doping.¹¹ Thus, in the case of $\text{NaFe}_{1-x}\text{Cu}_x\text{As}$, where no cT phase has been observed, it is natural to observe electron doping at low-

level substitution of Cu for Fe.

V. SUMMARY AND CONCLUSIONS

In conclusion, we have performed structural, transport, thermodynamic, and high pressure measurements on $\text{NaFe}_{1-x}\text{Cu}_x\text{As}$ single crystals. Enough carriers can be provided by Cu doping to map out a phase diagram similar to $\text{NaFe}_{1-x}\text{Co}_x\text{As}$. In underdoped region, Both the structural and SDW transition are monotonically suppressed by Cu doping. T_c and the superconducting shielding fraction are enhanced with the doping. Bulk superconductivity with $T_c = 11.5$ K is observed at optimally doped sample, and a metal-insulator transition is observed with further doping. Finally, insulating instead of metallic behavior in $\text{NaFe}_{1-x}\text{Co}_x\text{As}$ is observed in extremely overdoped non-superconducting samples. T_c is

obviously enhanced by pressure, but the T_c^{max} decreases with Cu concentration. The Hall measurements and comparison between Cu and Co doped NaFeAs phase diagrams indicate that Cu doping introduces electron into system, but the number of electron is far from $3x$ as predicted by rigid-band model.

Acknowledgements

This work is supported by the National Natural Science Foundation of China (Grants No. 11190021, 11174266, 51021091), the "Strategic Priority Research Program (B)" of the Chinese Academy of Sciences (Grant No. XDB04040100), the National Basic Research Program of China (973 Program, Grants No. 2012CB922002 and No. 2011CBA00101), and the Chinese Academy of Sciences.

-
- ¹ Y. Kamihara, T. Watanabe, M. Hirano, and H. Hosono, *J. Am. Chem. Soc.* **130**, 3296 (2008).
 - ² X. H. Chen, T. Wu, G. Wu, R. H. Liu, H. Chen, and D. F. Fang, *Nature (London)* **453**, 761 (2008).
 - ³ M. Rotter, M. Tegel, and D. Johrendt, *Phys. Rev. Lett.* **101**, 107006 (2008).
 - ⁴ A. S. Sefat, R. Jin, M. A. McGuire, B. C. Sales, D. J. Singh, and D. Mandrus, *Phys. Rev. Lett.* **101**, 117004 (2008).
 - ⁵ N. Ni, A. Thaler, J. Q. Yan, A. Kracher, E. Colombier, S. L. Bud'ko, P. C. Canfield and S. T. Hannahs, *Phys. Rev. B* **82**, 024519 (2010).
 - ⁶ S. Ideta, T. Yoshida, I. Nishi, A. Fujimori, Y. Kotani, K. Ono, Y. Nakashima, S. Yamaichi, T. Sasagawa, M. Nakajima, K. Kihou, Y. Tomioka, C. H. Lee, A. Iyo, H. Eisaki, T. Ito, S. Uchida, and R. Arita, *Phys. Rev. Lett.* **110**, 107007 (2013).
 - ⁷ Y. J. Yan, P. Cheng, J. J. Ying, X. G. Luo, F. Chen, H. Y. Zou, A. F. Wang, G. J. Ye, Z. J. Xiang, J. Q. Ma, and X. H. Chen, *Phys. Rev. B* **87**, 075105 (2013).
 - ⁸ M. Merz, P. Schweiss, P. Nagel, Th. Wolf, H. v. Löhneysen, and S. Schuppler, *arXiv*: 1306.4222.
 - ⁹ J. A. McLeod, A. Buling, R. J. Green, T. D. Boyko, N. A. Skorikov, E. Z. Kurmaev, M. Neumann, L. D. Finkelstein, N. Ni, A. Thaler, S. L. Bud'ko, P. C. Canfield, and A. Moewes, *J. Phys.: Condens. Matter* **24**, 215501 (2012).
 - ¹⁰ D. J. Singh, *Phys. Rev. B* **79**, 153102 (2009).
 - ¹¹ V. K. Anand, P. K. Perera, A. Pandey, R. J. Goetsch, A. Kreyssig, and D. C. Johnston, *Phys. Rev. B* **85**, 214523 (2012).
 - ¹² A. Thaler, H. Hodovanets, M. S. Torikachvili, S. Ran, A. Kracher, W. Straszheim, J. Q. Yan, E. Mun, and P. C. Canfield, *Phys. Rev. B* **84**, 144528 (2011).
 - ¹³ P. Cheng, B. Shen, F. Han, and H. H. Wen, *arXiv*: 1304.4568.
 - ¹⁴ D. R. Parker, M. J. P. Smith, T. Lancaster, A. J. Steele, I. Franke, P. J. Baker, F. L. Pratt, M. J. Pitcher, S. J. Blundell, and S. J. Clarke, *Phys. Rev. Lett.* **104**, 057007 (2010).
 - ¹⁵ A. F. Wang, X. G. Luo, Y. J. Yan, J. J. Ying, Z. J. Xiang, G. J. Ye, P. Cheng, Z. Y. Li, W. J. Hu, and X. H. Chen, *Phys. Rev. B* **85**, 224521 (2012).
 - ¹⁶ L. Y. Xing, X. C. Wang, Z. Deng, Q. Q. Liu, C. Q. Jin, *Physica C* in press.
 - ¹⁷ A. F. Wang, J. J. Ying, X. G. Luo, Y. J. Yan, D. Y. Liu, Z. J. Xiang, P. Cheng, G. J. Ye, L. J. Zou, Z. Sun, and X. H. Chen, *New J. Phys.* **15**, 043048 (2013).
 - ¹⁸ N. Spyrison, M. A. Tanatar, K. Cho, Y. Song, P. C. Dai, C. L. Zhang, and R. Prozorov, *Phys. Rev. B* **86**, 144528 (2012).
 - ¹⁹ S. L. Li, C. de la Cruz, Q. Huang, G. F. Chen, T. -L. Xia, J. L. Luo, N. L. Wang, and P. C. Dai, *Phys. Rev. B* **80**, 020504(R) (2009).
 - ²⁰ A. J. Williams, T. M. McQueen, V. Ksenofontov, C. Felser, and R. J. Cava, *J. Phys.: Condens. Matter* **21**, 305701 (2009).
 - ²¹ Tzu-Wen Huang, Ta-Kun Chen, Kuo-Wei Yeh, Chung-Ting Ke, Chi Liang Chen, Yi-Lin Huang, Fong-Chi Hsu, Maw-Kuen Wu, Phillip M. Wu, Maxim Avdeev, and Andrew J. Studer, *Phys. Rev. B* **82**, 104502 (2010).
 - ²² Stanislav Chadov, Daniel Schärfer, Gerhard H. Fecher, Claudia Felser, L. J. Zhang and D. J. Singh *Phys. Rev. B* **81**, 104523 (2010).
 - ²³ X. F. Wang, T. Wu, G. Wu, R. H. Liu, H. Chen, Y. L. Xie, and X. H. Chen, *New J. Phys.* **11**, 045003 (2009).
 - ²⁴ R. Klingeler, N. Leps, I. Hellmann, A. Popa, U. Stockert, C. Hess, V. Kataev, H. -J. Grafe, F. Hammerath, G. Lang, S. Wurmehl, G. Behr, L. Harnagea, S. Singh, and B. Büchner, *Phys. Rev. B* **81**, 024506 (2010).
 - ²⁵ G. M. Zhang, Y. H. Su, Z. Y. Lu, Z. Y. Weng, D. H. Lee, and T. Xiang, *Europhys. Lett.* **86**, 37006 (2009).
 - ²⁶ M. M. Korshunov, I. Eremin, D. V. Efremov, D. L. Maslov, and A. V. Chubukov, *Phys. Rev. Lett.* **102**, 236403 (2009).
 - ²⁷ Z. J. Xiang, X. G. Luo, J. J. Ying, X. F. Wang, Y. J. Yan, A. F. Wang, P. Cheng, G. J. Ye, and X. H. Chen, *Phys. Rev. B* **85**, 224527 (2012).
 - ²⁸ G. H. Cao, S. Jiang, X. Lin, C. Wang, Y. K. Li, Z. Ren, Q. Tao, C. M. Feng, J. H. Dai, Z. A. Xu, and F. C. Zhang, *Phys. Rev. B* **79**, 174505 (2009).

- ²⁹ F. Rullier-Albenque, D. Colson, A. Forget, and H. Alloul, *Phys. Rev. Lett.* **103**, 057001 (2009).
- ³⁰ E. Arushanov, S. Levchenko, G. Fuchs, B. Holzapfel, S. L. Drechsler, and L. Schultz, *J. Supercond. Nov. Magn.* **24**, 2285 (2011).
- ³¹ T. R. Chien, Z. Z. Wang, and N. P. Ong, *Phys. Rev. Lett.* **67**, 2088 (1991).
- ³² C. H. Wang, G. Y. Wang, T. Wu, Z. Feng, X. G. Luo, and X. H. Chen, *Phys. Rev. B* **72**, 132506 (2005).
- ³³ S. L. Bud'ko, N. Ni, and P. C. Canfield, *Phys. Rev. B* **79**, 220516 (2009).
- ³⁴ J. S. Kim, G. R. Stewart, S. Kasahara, T. Shibauchi, T. Terashima, and Y. Matsuda, *J. Phys.: Condens. Matter* **23**, 222201 (2011).
- ³⁵ G. R. Stewart, *Rev. Mod. Phys.* **83**, 1589 (2011).
- ³⁶ P. Cai, X. D. Zhou, W. Ruan, A. F. Wang, X. H. Chen, D. H. Lee, and Y. Y. Wang, *Nat. Commun.* **4**, 1596 (2013).
- ³⁷ A. F. Wang, Z. J. Xiang, J. J. Ying, Y. J. Yan, P. Cheng, G. J. Ye, X. G. Luo, and X. H. Chen, *New J. Phys.* **14**, 113043 (2012).
- ³⁸ G. F. Chen, W. Z. Hu, J. L. Luo, and N. L. Wang, *Phys. Rev. Lett.* **102**, 227004 (2009).
- ³⁹ N. Ni, M. E. Tillman, J. -Q. Yan, A. Kracher, S. T. Hannahs, S. L. Bud'ko, and P. C. Canfield, *Phys. Rev. B* **78**, 214515 (2008).
- ⁴⁰ H. Q. Yuan, J. Singleton, F. F. Balakirev, S. A. Baily, G. F. Chen, J. L. Luo, and N. L. Wang, *Nature* **457**, 565 (2009).
- ⁴¹ M. H. Fang, J. H. Yang, F. F. Balakirev, Y. Kohama, J. Singleton, B. Qian, Z. Q. Mao, H. D. Wang, and H. Q. Yuan, *Phys. Rev. B* **81**, 020509(R) (2010).
- ⁴² J. Jaroszynski, F. Hunte, L. Balicas, Y. -j. Jo, I. Raičević, A. Gurevich, D. C. Larbalestier, F. F. Balakirev, L. Fang, P. Cheng, Y. Jia, and H. H. Wen, *Phys. Rev. B* **78**, 174523 (2008).
- ⁴³ F. Hardy, T. Wolf, R. A. Fisher, R. Eder, P. Schweiss, P. Adelman, H. v. Löhneysen, and C. Meingast, *Phys. Rev. B* **81**, 060501(R) (2010).
- ⁴⁴ S. J. Zhang, X. C. Wang, Q. Q. Liu, Y. X. Lv, X. H. Yu, Z. J. Lin, Y. S. Zhao, L. Wang, Y. Ding, H. K. Mao, and C. Q. Jin, *Europhys. Lett.* **88**, 47008 (2009).
- ⁴⁵ H. Wadati, I. Elfimov, and G. A. Sawatzky, *Phys. Rev. Lett.* **105**, 157004 (2010).
- ⁴⁶ T. Berlijn, C. H. Lin, W. Garber, and W. Ku, *Phys. Rev. Lett.* **108**, 207003 (2012).
- ⁴⁷ K. Nakamura, R. Arita, and H. Ikeda, *Phys. Rev. B* **83**, 144512 (2011).
- ⁴⁸ M. G. Kim, J. Lamsal, T. W. Heitmann, G. S. Tucker, D. K. Pratt, S. N. Khan, Y. B. Lee, A. Alam, A. Thaler, N. Ni, S. Ran, S. L. Bud'ko, K. J. Marty, M. D. Lumsden, P. C. Canfield, B. N. Harmon, D. D. Johnson, A. Kreyssig, R. J. McQueeney, and A. I. Goldman, *Phys. Rev. Lett.* **109**, 167003 (2012).